Electronic Supplementary Material (ESI) for Chemical Communications

Supporting Information

Asymmetric pyrene derivatives for organic field-effect transistors

Lukas Zöphel, Dirk Beckmann, Volker Enkelmann, Dennis Chercka, Ralph Rieger and Klaus Müllen*[a]

[a] *Max-Planck-Institute for Polymer Research*
Ackermannweg 10, 55128 Mainz (Germany)
Fax: (+49)6131-379-100
E-mail: muellen@mpip-mainz.mpg.de

Synthesis

Commercially available reagents were used without further purification unless otherwise stated. Melting points were determined on a Büchi hot stage apparatus and are uncorrected. Fielddesorption mass spectra were obtained on a VG Instruments ZAB 2-SE-FPD spectrometer. ^{1}H-NMR and ^{13}C-NMR experiments were recorded in the listed deuterated solvents on a Bruker AVANCE 300 or a Bruker AVANCE 500 spectrometer. The deuterated solvent was used as an internal standard. Mass spectra were obtained using FD on a VG Instruments ZAB 2 SE-FPD. Elemental analysis of solid samples was carried out on a Foss Heraeus Vario EL.

4,5-Dibromo-9,10-diketopyrene (3)

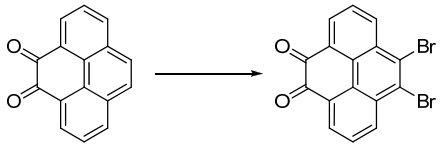

2 3

To a solution of 4,5-diketopyrene (2.0 g, 8.61 mmol) in 20 ml concentrated sulfuric acid N-bromosuccinimide (3.07 g, 17.25 mmol) was added and stirred for 4 hours at room temperature. The reaction mixture was precipitated in 2 L H_2O/ice, collected by filtration, washed with water and dried under high vacuum to give **4** in quantitative yield as bright brownish solid.

^{1}H NMR (500 MHz, DMSO-d_6, 120°C) δ/ppm 8.72 (d, J = 8.3 Hz, 2H), 8.47 (d, J = 7.4 Hz, 2H), 7.98 (t, J = 7.9 Hz, 2H).

^{13}C NMR (126 MHz, DMSO-d_6, 120°C) δ/ppm 178.07, 134.59, 130.24, 130.14, 129.45, 128.99, 127.55, 125.20.

Mp = 360 °C (decomposition)

Elemental analysis (%) calculated $C_{16}H_6Br_2O_2$: C, 49.27; H, 1.55; Found: C, 49.41; H, 1.73;

4,5-Dibromo-9,10-dimethoxypyrene (4)

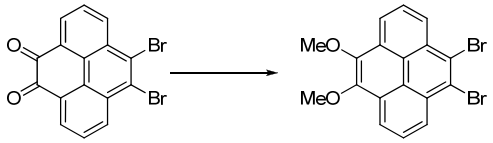

3 4

4,5-Dibromo-9,10-diketopyrene (1.0 g, 2.56 mmol), Bu_4NBr (0.578 g, 1.79 mmol) and $Na_2S_2O_4$ (1.34 g, 7.7 mmol) were suspended in 16 ml THF and 9 ml water. Me_2SO_4 (1.8 g, 13.3 mmol) was added followed by 7 ml 4.5 M aqueous KOH and the reaction mixture was stirred capped with a condenser at 40°C overnight. DCM was added, the organic phase was extracted, dried over $MgSO_4$ and the organic solvent were removed under vacuum. Column chromatography on silica with PE:DCM 1:1, followed by crystallization from Ethanol gave **5** (0.695 g, 1.66 mmol) as colorless crystals in 65 % yield.

^{1}H NMR (300 MHz, CD_2Cl_2) δ/ppm 8.66 (dd, *J* = 8.0, 1.0 Hz, 2H), 8.59 (dd, *J* = 7.9, 0.9 Hz, 2H), 8.13 – 8.05 (m, 2H), 4.20 (s, 6H).

^{13}C NMR (75 MHz, CD_2Cl_2) δ/ppm 144.96, 130.88, 129.14, 127.71, 127.12, 126.74, 122.75, 121.73, 61.67.

Mp = 176 °C

MS (FD, 8 kV) m/z = 422.2 g/mol - calculated: 420.1 g/mol for $C_{18}H_{12}Br_2O_2$

Elemental analysis (%) calculated $C_{18}H_{12}Br_2O_2$: C, 51.46; H, 2.88; Found: C, 51.07; H, 2.89

4,5-Dimethoxy-9,10-di(thien-2-yl)pyrene (5)

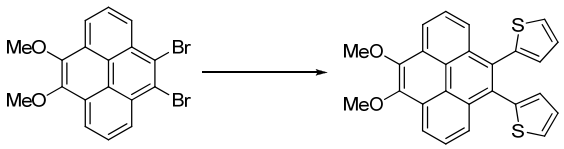

4 5

A solution of 4,5-dibromo-9,10-dimethoxypyrene (0.3 g, 0.714 mmol) in 10 ml dry toluene was degassed with argon for 15 minutes. $Pd(PPh_3)_4$ (0.025 g, 0.021mmol) and 2-(tributylstannyl)thiophene (0.8 g, 2.14 mmol) were added, degassed for additional 5 minutes und refluxed under argon overnight. The organic solvent was removed under reduced pressure and the residue was purified over silica column PE: DCM 2:1 and crystallized from ethanol to give **6 (**0.210 g, 0.492 mmol) as slightly yellow solid in 69% yield.

^{1}H NMR (300 MHz, CD_2Cl_2) δ/ppm 8.55 (dd, *J* = 6.8, 2.1 Hz, 2H), 8.04 – 7.96 (m, 4H), 7.43 (dd, *J* = 4.9, 1.5 Hz, 2H), 7.11 – 7.06 (m, 4H), 4.23 (s, 6H).

^{13}C NMR (75 MHz, CD_2Cl_2) δ/ppm 145.13, 140.17, 133.39, 132.16, 130.15, 128.78, 127.01, 126.82, 126.79, 124.87, 123.10, 120.61, 61.65.

Mp = 182 °C

MS (FD, 8 kV) m/z = 425.1 g/mol - calculated: 426.1 g/mol for $C_{26}H_{18}O_2S_2$

Elemental analysis (%) calculated $C_{26}H_{18}O_2S_2$: C, 73.21; H, 4.25; S, 15.03; Found: C, 73.07; H, 4.16; S, 14.81

4,5-(Benzo[1',2'-b';4'',3''-b'']dithieno)-9,10-dimethoxy pyrene (1)

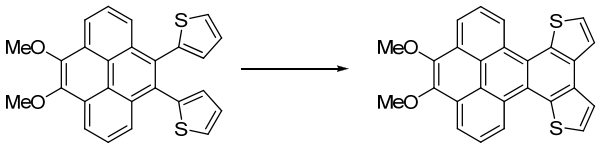

5 **1**

A solution of 4,5-dimethoxy-9,10-di-(thien-2-yl)pyrene (0.255 g, 0.598 mmol) and iodine (0.303 g, 1.196 mmol) in 255 ml toluene was degassed with argon for 15 minutes and irradiated in a quartz tube at 300 nm overnight. The reaction mixture was washed with aqueous Na_2SO_3 solution, dried over $MgSO_4$ and the organic solvents were removed. Crystallization from ethanol gave **1 (**0.120 g, 0.283 mmol) as slightly yellow crystals in 47% yield.

^{1}H NMR (300 MHz, CD_2Cl_2) δ/ppm 9.59 (dd, *J* = 8.1, 0.8 Hz, 2H), 8.63 (dd, *J* = 7.9, 0.8 Hz, 2H), 8.21 (t, *J* = 8.0 Hz, 2H), 8.01 (d, *J* = 5.6 Hz, 2H), 7.85 (d, *J* = 5.5 Hz, 2H), 4.25 (s, 6H).

^{13}C NMR (75 MHz, CD_2Cl_2) δ/ppm 144.85, 136.14, 134.30, 129.57, 129.10, 128.07, 126.83, 125.90, 123.97, 122.91, 122.80, 120.87, 61.68.

Mp = 198 °C

MS (FD, 8 kV) m/z = 421.6 g/mol - calculated: 424.1 g/mol for $C_{26}H_{16}O_2S_2$

Elemental analysis (%) calculated $C_{26}H_{16}O_2S_2$: C, 73.56; H, 3.80; S, 15.11; Found: C, 73.01; H, 3.87; S, 15.04

Crystal packing of compound 1

Data collections for the crystal-structure analysis were performedon a Nonius KCCD diffractometer equipped with a Cryostream cooler with graphite monochromated MoKa radiation.

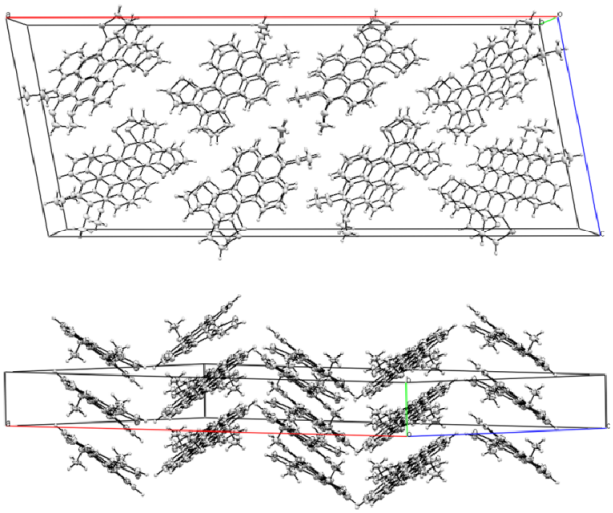

Figure S1: Packing diagrams of **1**: (top) view parallel to b, highlighting the π-π stacking; (bottom) view in right angle to b, showing the herringbone packing motive

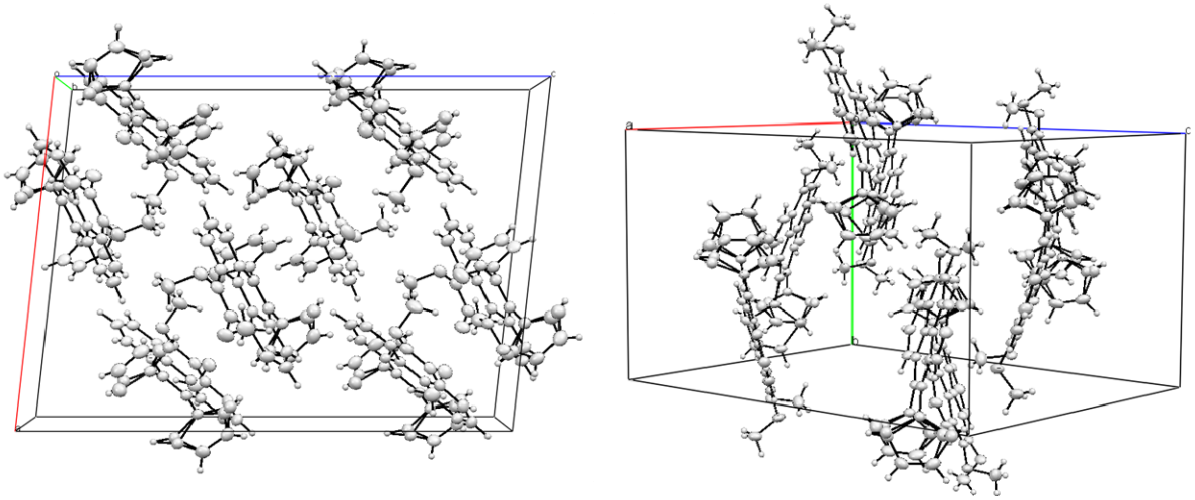

Figure S2: Packing diagrams of **5**: (left) view parallel to b; (right) view in right angle to b

UV-vis Spectroscopy of compounds 1 and 5

The spectra are recorded in a 10^{-5} M solution in THF on a Perkin-Elmer Lambda 100 spectrophotometer. Photoluminescence in 10^{-5} M THF solution are measured on a SPEX-Fluorolog II (212) instrument.

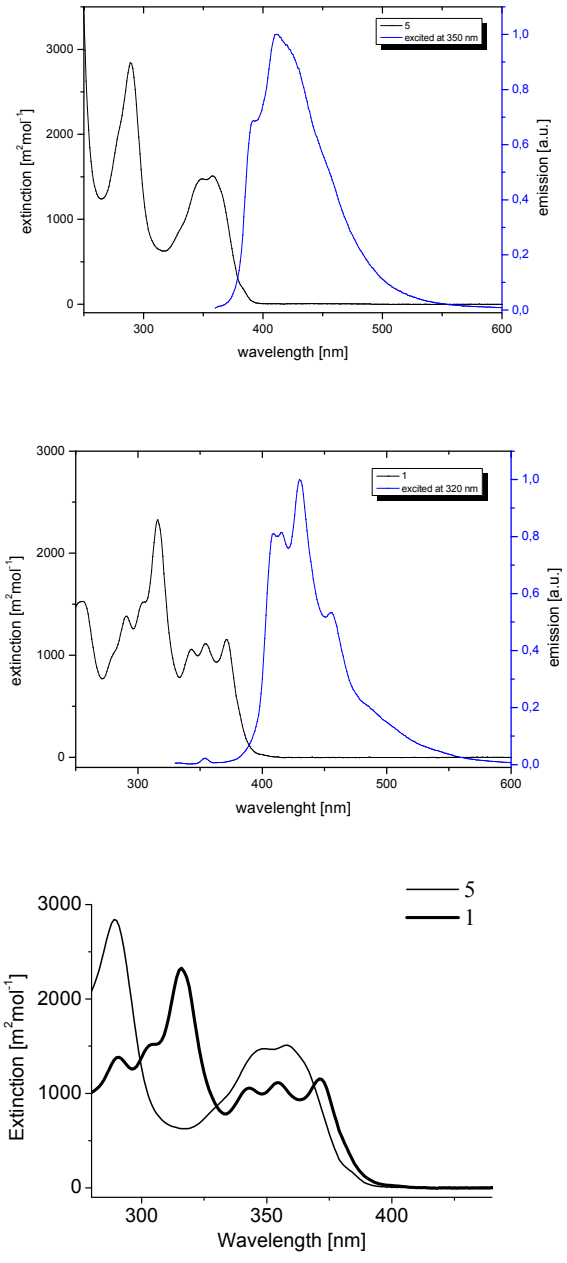

Figure S3: Absorption and photoluminescenz spectra of **5** and **1**

CV measurements of compounds 1 and 5

Cyclic volatammetry was measured on a Princeton Applied Research Parstat 2273 instrument with anhydrous dichloromethane under argon atmosphere. n-Bu_4NPF_6 was used as conductive salt at a concentration of 0.1 mol/l. Ferrocene was added as internal standard (1 mM). The peaks were calibrated according to the oxidation peak of ferrocene for HOMO level calculation. The voltage was ramped by 100 mV/s. Half-step potentials were used for the evaluation. No reduction peaks were observed.

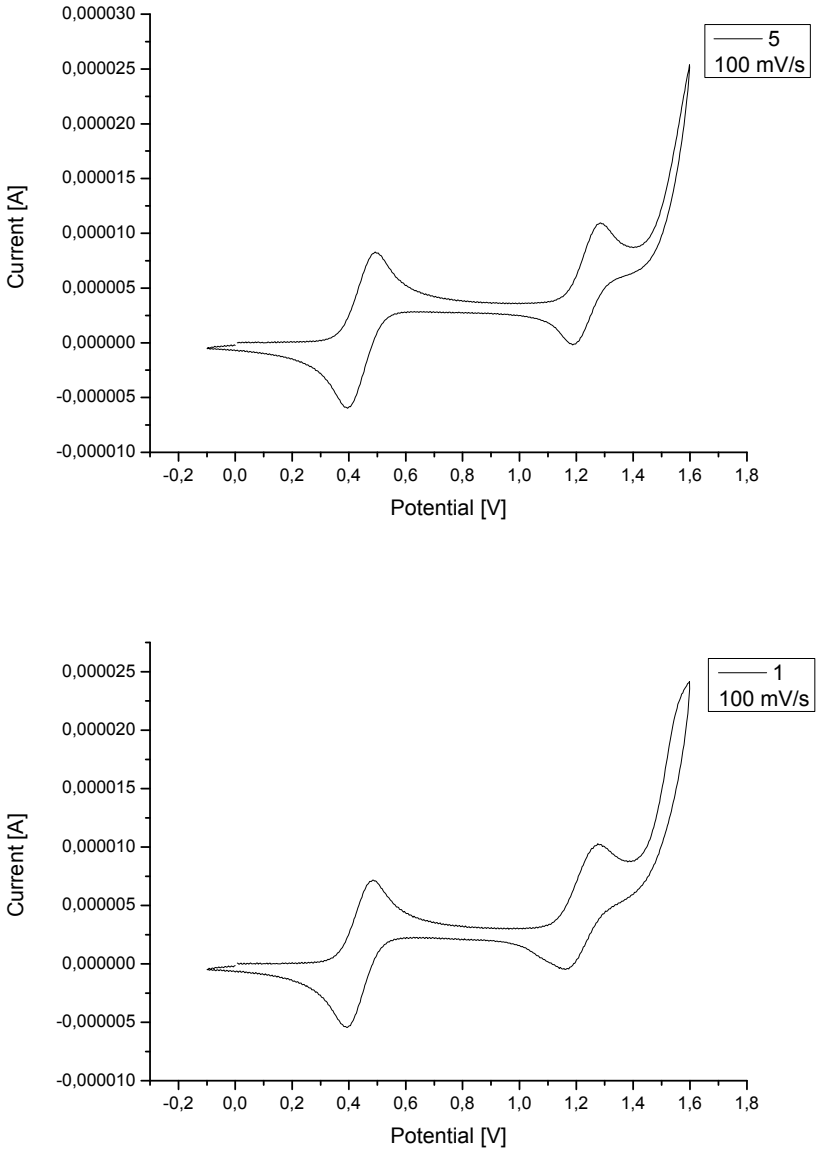

Figure S4: CV of **5** and **1**

Field-Effect Transistors

Device fabrications and evaluations: For all devices, heavily doped silicon wafers with a 200 nm thick thermally grown silicon dioxide layer have been used as substrates. For the bottom gate, top contact OFETs, source and drain electrodes with channel geometries of W/L = 20 were defined by a shadow mask, followed by Au evaporation to a height of 100 nm. In order to avoid interface trapping the silicon dioxide was modified by using hexamethyldisilazane (HMDS) processed from the gas phase at 120°C resulting in appropriate contact angles of 93° against deionized water. For the solution processing of the semiconductor the common organic solvent toluene has been used. A schematic of the dip-coating procedure is illustrated in Figure S5. The 2 mg/ml semiconductor toluene solution was filled up to 11 mm in a cylindrical glass container with a diameter of 12 mm and a height of 39 mm. The dip-coated film was grown by completely immersing the transistor substrates (10x10 cm in size) in this solution and by slowly taking the sample out at a rate of 0.5 µm s^{-1} using an electrically controlled engine. The dip-coating direction is highlighted by the red arrow in Figure S5 and S6. The film appeared by eye above the solution meniscus of about 1 mm. The average thickness of the dip-coated films is about 1 µm. The whole experiment was performed in environmental conditions (rh = 33,0 ± 3,6 %; T = 20,7 ± 2,2 °C). The transistors were completed by evaporating source and drain electrodes without any previous drying of the as-cast films.

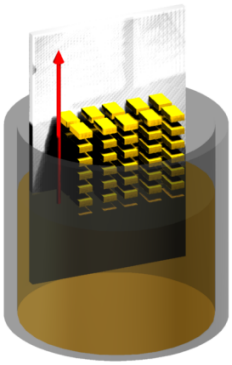

Figure S5: Schematic presentation of the dip-coating procedure. The red arrow highlights the coating direction. The yellow patterns indicate arranged molecules.

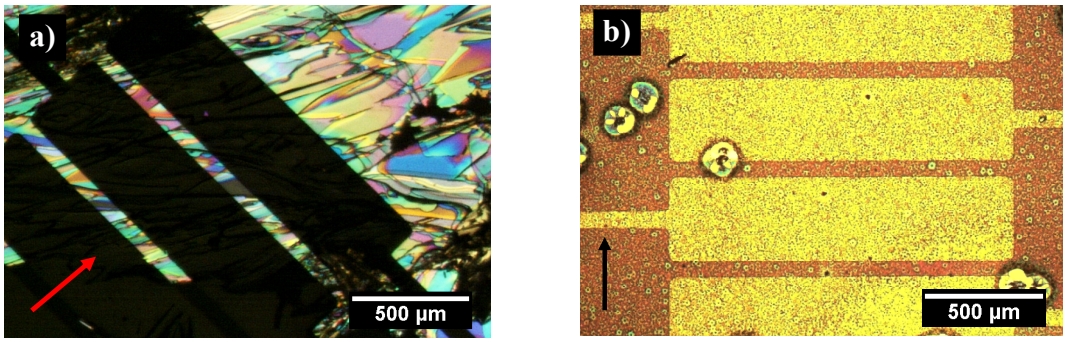

Figure S6. Film formation of dip-coated **1** (a) and **5** (b) on HMDS-treated silicon dioxide insulator in a bottom gate, top contact transistor configuration. The images were taken at a) crossed polarizer/analyzer and b) parallel polarizer/analyzer (since the polarized image of **5** based films appeared black). The arrows demonstrate the dip-coating direction.

The transistor characteristics were studied under exclusion of UV-light at room temperature inside a nitrogen filled glovebox with an oxygen and humidity level below 0.1 ppm. The device characteristics have been measured with a Keithley 4200 semiconductor characterization system

The charge carrier mobilities were calculated via

$$I_{SD,sat} = \frac{W}{2L}\mu_{sat}C_i(V_{SG} - V_T)^2$$

with the current in the saturation region $I_{SD,sat}$, channel width W, channel length L (W/L = 20), capacitance per unit area of the gate insulator C_i = 2.6 x 10^{-8} Fcm^{-2}, the saturated charge-carrier field-effect mobility μ_{sat}, and the threshold voltage V_T.

In addition to the main publication text, typical transfer (a) and output (b) curves of dip-coated **1** transistors are summarized in Figure S7. Comparing the transistor transfer and output curves a current drop of more than one decade appears that can be attributed to either charge carrier trapping (in spite of the dielectric's surface modification with HMDS) or structural changes which can be of molecular (degradation) or supramolecular (rearranging) nature. It is assumed that the off-current regime from 0 V to -8 V corresponds to the same mechanism, since the drain current increased linearly between the drain potential of - 8 and - 25 V and

contact resistance problems had led to a sub-linear increase. An educated explanation based on facts requires further tests concerning bias stress dependent charge carrier trapping and structural alteration but cannot be provided at this time.

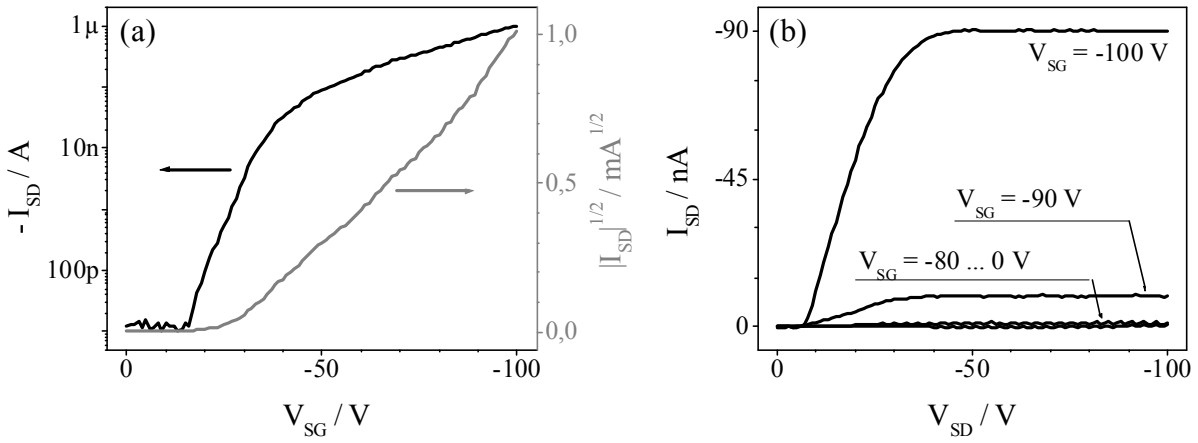

Figure S7. Typical transfer (a) and output (b) characteristics of dip-coated 1 transistors.

Film x-ray: X-ray diffraction (XRD) measurements were recorded on a Siemens D-500 powder diffractometer (Cu-Ka: 1.541 Å) with scan rate of 0.1°/20 s. The diffractrogram is given in Figure S8. The calculated distance a = 2.27 nm fits very well to the crystal structure date (compare Figure S9) indicating effective charge carrier transport within the device plane from source to drain electrodes.

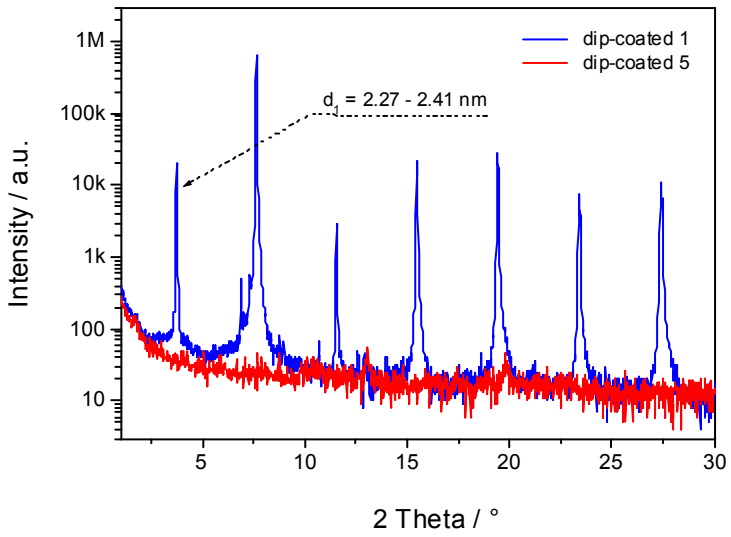

Figure S8. X-ray diffraction in reflection mode for the dip-coated film of **1** (blue) and **5** (red). $2\Theta_1 = 3.66 – 3.89°$ corresponds to an out-of-plane spacing $d_1 = 2.27 – 2.41$ nm in the **1** based film.

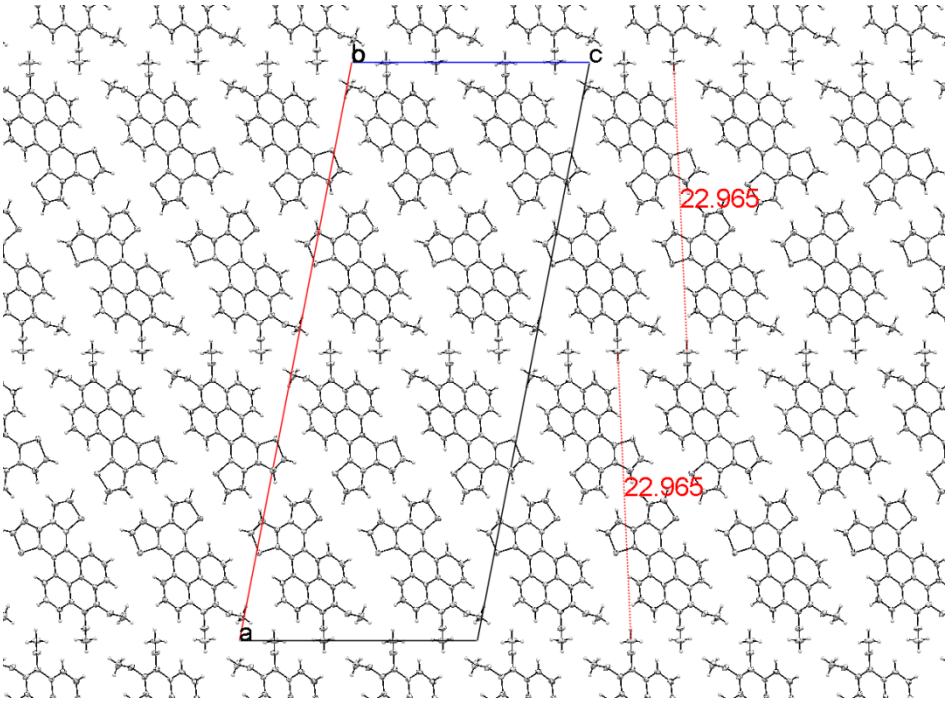

Figure S9: Organization of **1** in the solution processed thin layer on the substrate.

Electronic Supplementary Material (ESI) for Chemical Communications

DFT Calculations of compounds 1 and 5

Compound 5

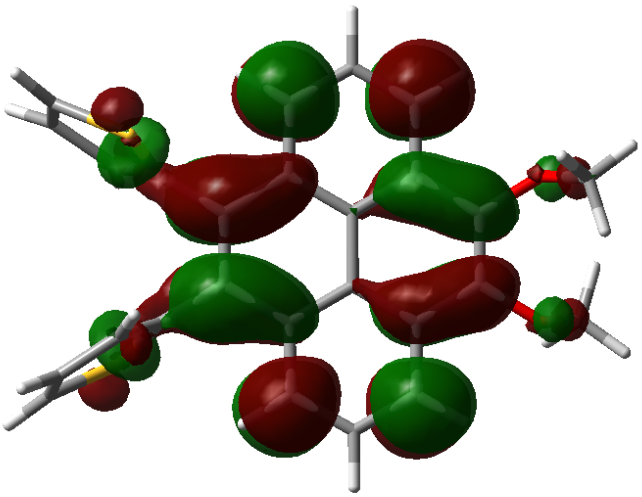

LUMO -1.93 eV
-0.071 h

band gap 3.62

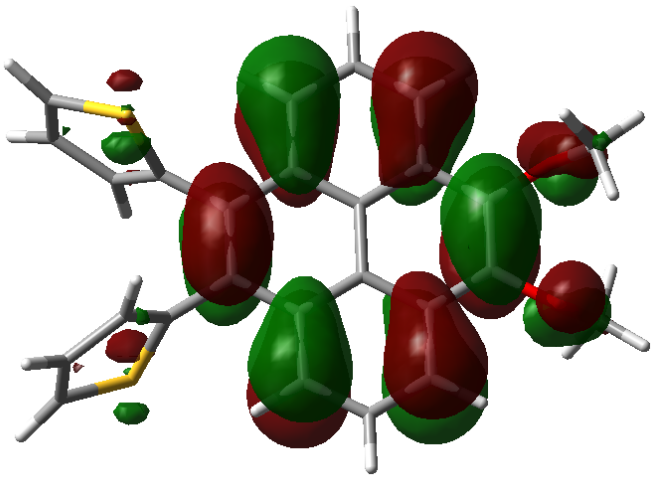

HOMO -5.55
-0.204 h

Compound 1

LUMO -1.96 eV
-0.072 h

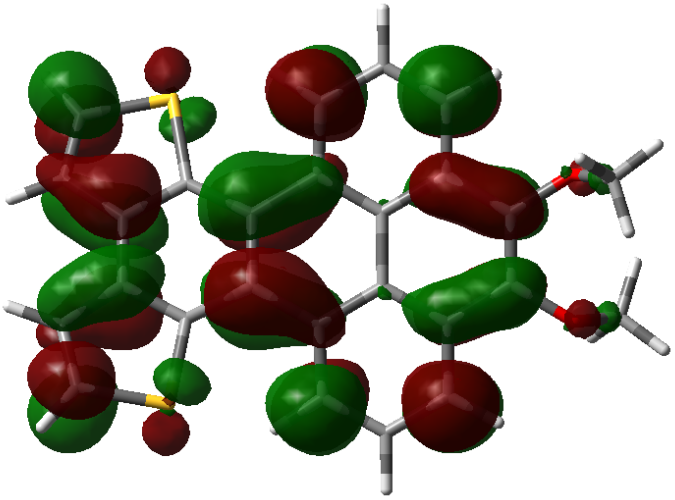

band gap 3.51

HOMO -5.47 eV
-0.201 h